

# Distribution and Apparent Decline of Aspen (*Populus tremuloides*) in the Broader Lake Tahoe Area: A Four-Decade Assessment

Prepared by:

Joseph A. E. Stewart, Department of Plant Sciences, UC Davis

Jonathan W. Long, Pacific Southwest Region, US Forest Service



Joseph Stewart

Suggested Citation:

Stewart J.A.E. & Long J.W. 2024. Distribution and Apparent Decline of Aspen (*Populus tremuloides*) in the Broader Lake Tahoe Area: A Four-Decade Assessment. *Tahoe Science Advisory Council (TSAC)*, Incline Village, NV.

## Table of Contents

<i>Abstract</i> .....	2
<i>Introduction</i> .....	2
<i>Results</i> .....	3
Spatial Models.....	3
Spatiotemporal Models .....	7
<i>Discussion and Management Implications</i> .....	11
<i>Methods</i> .....	13
Sample Design & Data Collection.....	13
Reflectance Data.....	18
Model Parameterization .....	20
<i>Contributors</i> .....	22
<i>Supplementary Materials</i> .....	22
<i>References</i> .....	23

# Abstract

We used machine learning models to produce remotely sensed maps of aspen (*Populus tremuloides*) percent cover in the broader Lake Tahoe area (BLTA). Aspen is an important ecological and cultural resource both sensitive to and dependent on wildfire, and also vulnerable to climate change. Elsewhere in its range aspen declines have been well documented. More information on where aspen are and how aspen cover has changed over time is needed to inform management. Our ensemble model of aspen cover over the past decade (2014–2023) performed well in cross-validated metrics of predictive performance (e.g.,  $R^2 = 0.81$ ). The maps provide a more accurate and detailed view of the distribution of aspen in our area compared with previous maps that delineated aspen presence but did not assess levels of cover. Model outputs indicate that aspen cover has declined in our study area over the past 40 years. This result is consistent across several distinct versions of our models, appears to be robust to potential sources of statistical bias, and is supported by multiple lines of outside evidence. Across the BLTA we provide an initial estimate that aspen cover has declined by about 26% (95% CI: 9–39%) over the 1984–2023 period. A greater focus on restoration treatments, such as prescribed fire, strategic management of naturally ignited fires, and targeted thinning of conifers overtopping aspen, could slow or reverse apparent aspen declines in our region. Detailed maps, such as our product, can serve to inform strategic and adaptive management.

# Introduction

Hardwood communities are an important ecological and cultural resource both sensitive to and dependent on wildfire, and also vulnerable to climate change. The Tahoe Regional Planning Agency has adopted an “environmental threshold” for riparian hardwoods in the basin through various policies and restoration projects, and it has sought to map trends over time and in response to restoration treatments targeting aspen (*Populus tremuloides*) communities. Similarly, the Land and Resource Management Plan for the Lake Tahoe Basin Management Unit prioritized a monitoring question, “What is our progress towards maintaining and improving willow and aspen habitats within the Basin?” Existing vegetation maps for the Tahoe Basin have deficiencies in their resolution, accuracy, and/or temporal update cycle that limit their utility in tracking the condition of existing hardwood stands. Updating these maps and providing accurate quantification of hardwoods has been identified as a management need. This project builds on recent regional work to build high-resolution maps of aspen stands in the Tahoe Basin.

# Results

## Spatial Models

Our remotely sensed estimate of the area of the Lake Tahoe Basin Management Unit (hereafter referred to simply as “the basin” or LTBMU) with at least 10% aspen cover over the period 2014–2023 was 886 ha (0.34% of terrestrial area). We estimate that 166 ha had at least 50% aspen cover during this period (0.06% of the terrestrial area in the basin). Aspen cover was higher over our entire study area, the Broader Lake Tahoe Area (BLTA), defined as the basin buffered by 20-km (Fig 1). We estimate the area of the BLTA with at least 10% and 50% aspen cover are 3,658 ha and 872 ha, respectively (0.43% and 0.10% of terrestrial area, Fig 2). These estimates are derived from our ensemble machine learning model version 4.6.LS4to9.Ensemble.T02, also referred to simply as “ensemble model” elsewhere in this report. They reflect estimated aspen cover within 900-m<sup>2</sup> Landsat-aligned grid cells. Estimates of “cover” refer to percent cover from above (PCFA), the percent cover visible from directly overhead, visible to satellites in low earth orbit. The term “cover” is used interchangeably with PCFA elsewhere in this report.

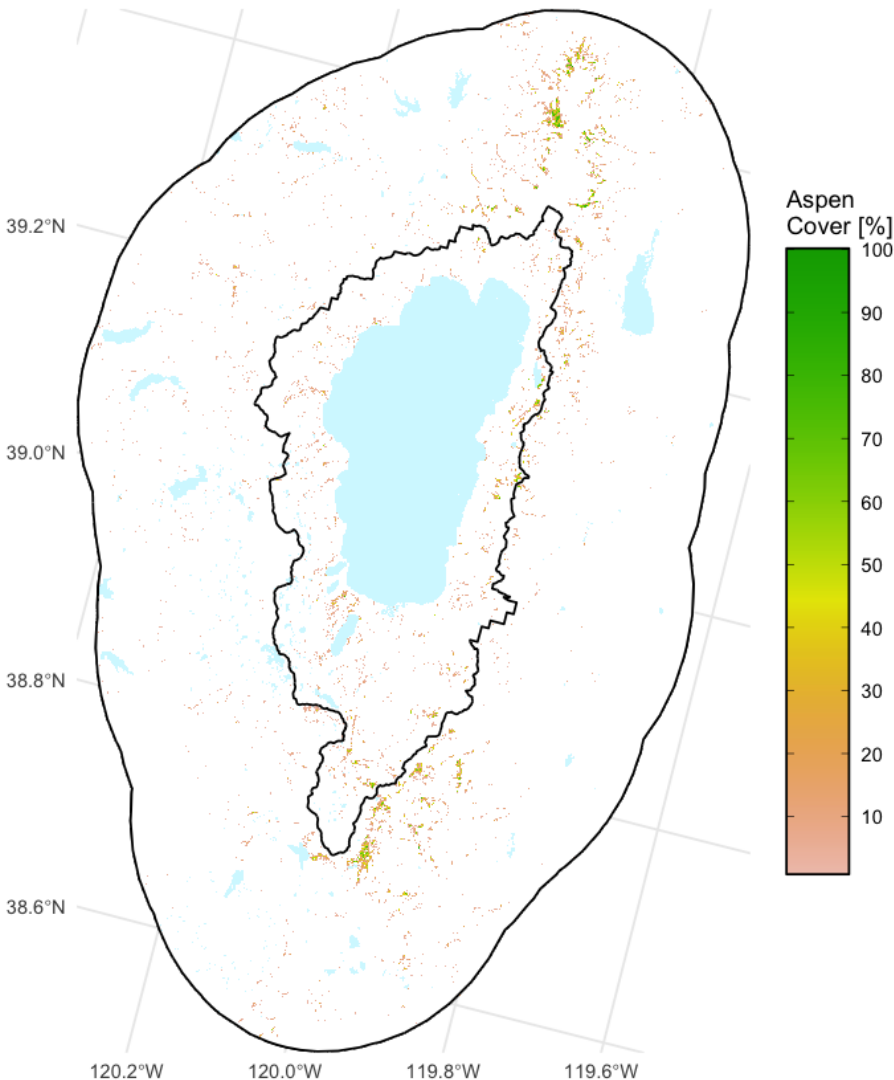


**Fig 1.** Map of aspen cover for the period 2014–2023 as estimated by our ensemble model. The external boundary is the broader Lake Tahoe area. The internal boundary is the Lake Tahoe Basin Management Unit. Lakes are shown in light blue.

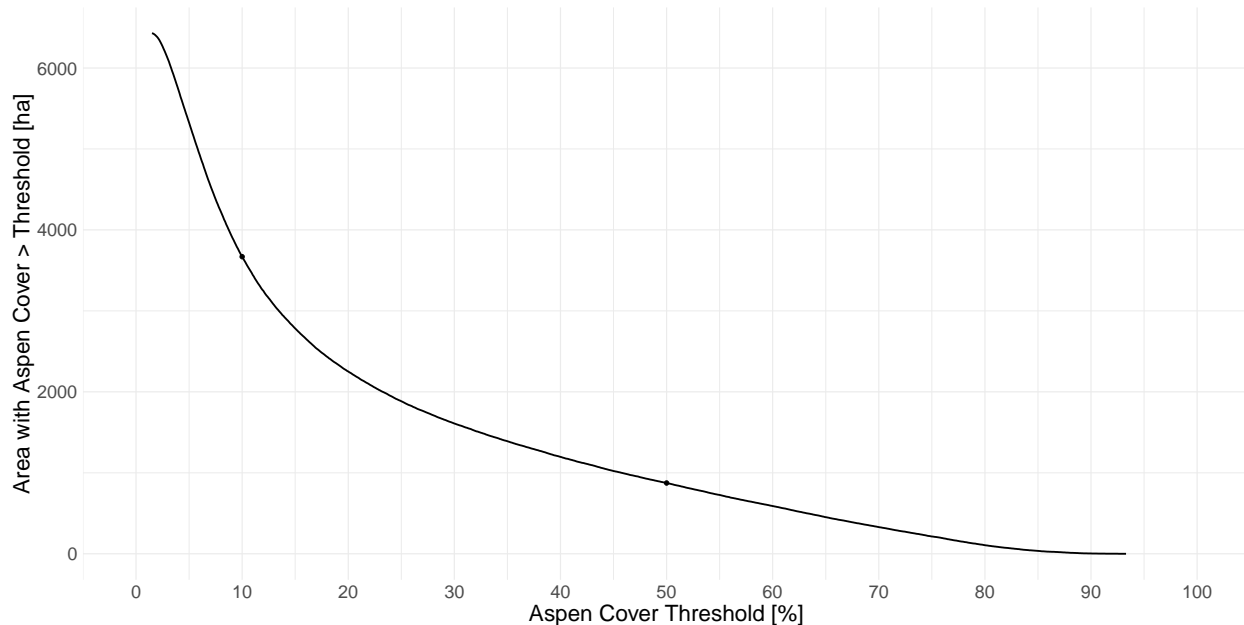


**Fig 2.** Area of the broader Lake Tahoe area with aspen cover above threshold levels, as estimated by our ensemble model for the period 2014–2023. Areas with sparse scattered aspen trees (e.g., 10–20% aspen cover) appear to be more extensive than areas with high aspen cover (e.g., > 80% aspen cover). The area with greater than 10% and 50% aspen cover are shown with small dots. Estimates of the area with less than about 10% aspen cover may be less reliable, as the frequency of commission and omission errors appears to be more prevalent below this threshold.

Our models of aspen cover over the 10-year period 2014–2023 performed well in cross-validated metrics of predictive performance (Table 1). Ensemble and extreme gradient boosting (XGB) models were trained and evaluated on 82,967 900-m<sup>2</sup> Landsat-aligned plots, including 1,108 surveyed plots, 41,874 background plots, and 39,985 NPP plots (see methods). Survey plots with disturbance events between the survey date and model period (2014–2023) were excluded. Maxent (ME) models were trained and evaluated on a smaller dataset, consisting of plots where each seasonal period had at least one unobstructed satellite observation of spectral reflectance over the full model period.

The coefficient of determination for our ensemble model was 0.81 (Table 1). The ensemble model had the best performance in terms of coefficient of determination, root mean square error, and Brier Score, while the XGB model had the highest performance in terms of mean absolute error and log loss. Plots of observed vs predicted performance indicate the XGB and ME models each had their own strengths and weaknesses. XGB had better performance distinguishing areas with aspen from areas without aspen. ME had better accuracy and less bias distinguishing the level of aspen cover. Missing (*i.e.*, obstructed) spectral data resulted in the ME model being unable to estimate cover in about 1.4% of the terrestrial area within our study region. To capture the best aspects of both models we composed an ensemble model with aspen cover calculated as  $\text{mean}(P_{XBG}, P_{ME}) \cdot (P_{XBG} \geq 2)$ , where  $P_{XBG}$  and  $P_{ME}$  are percent aspen cover, as estimated by the two component models. The 2% threshold applied to the XGB model was set by examining aerial imagery, reliability diagrams, and performance metrics, and driving around the BLTA with binoculars, attempting to balance the resulting levels of

commission and omission errors. The resulting ensemble model has strong overall performance, with a notable bias toward underpredicting aspen cover in plots with > 80% aspen cover (Fig 3).

**Table 1.** Cross-validated predictive performance of top performing models of aspen cover for the period 2014-2023. Ensemble and XGB models were trained and evaluated on 82,967 900-m<sup>2</sup> Landsat-aligned plots, including 1,108 surveyed plots, 41,874 background plots, and 39,985 NPP plots. Survey plots with disturbance events between the survey date and model period (2014–2023) were excluded. ME models were trained and evaluated on a smaller dataset, consisting of plots where no seasonal periods were completely obstructed over the full model period. Ensemble models use the simple mean of XGB and ME predictions.

Model	R <sup>2</sup>	MAE	RMSE	Log Loss	Brier Score
4.6.LS4to9.Ensemble.T02	0.8120	0.0051	0.0255	0.0097	0.0006
4.6.LS4to9.XGB	0.7813	0.0037	0.0275	0.0087	0.0008
4.6.LS4to9.ME	0.7989	0.0230	0.0517	0.0408	0.0027

Informal field surveys (driving, walking, bicycling, binoculars) conducted from June–October 2024 by JAES and JWL, also suggest our ensemble model has strong overall performance. The boundaries of large aspen stands are depicted with remarkable detail. The model successfully detects the presence of aspen that are intermixed with a multitude of other plant species and understory conditions. Notably, the model often fails to detect low levels of aspen cover in more urban or suburban environments (*e.g.*, parking lots, irrigated lawns, denser buildings); this is unsurprising given the data used to train the model came mostly from less disturbed native ecosystems. Omission errors in 900-m<sup>2</sup> pixels with greater than about 10% aspen cover from above appear to be relatively uncommon. Below this level omission errors become more common. We observed many instances where the model failed to detect low levels of aspen cover (*e.g.*, a single large aspen tree within a pixel, sparse saplings typically totaling less than about 10% cover within a pixel). As expected, when satellite views of aspen are largely obstructed by taller trees (*i.e.*, high understory cover but low cover from above) the model’s ability to detect aspen is hampered. Commission errors typically consist of the model estimating low levels of aspen cover in areas dominated by allied species and vegetation types (*e.g.*, montane riparian, alder, cottonwood, willows). Commission errors appear to be relatively uncommon in areas the model estimated have greater than about 10% aspen cover. Providing our model with additional training data—spanning a wider range of adjacent vegetation compositions—would improve its overall performance. In particular, the model would benefit from additional survey data from areas dominated by other montane riparian species.

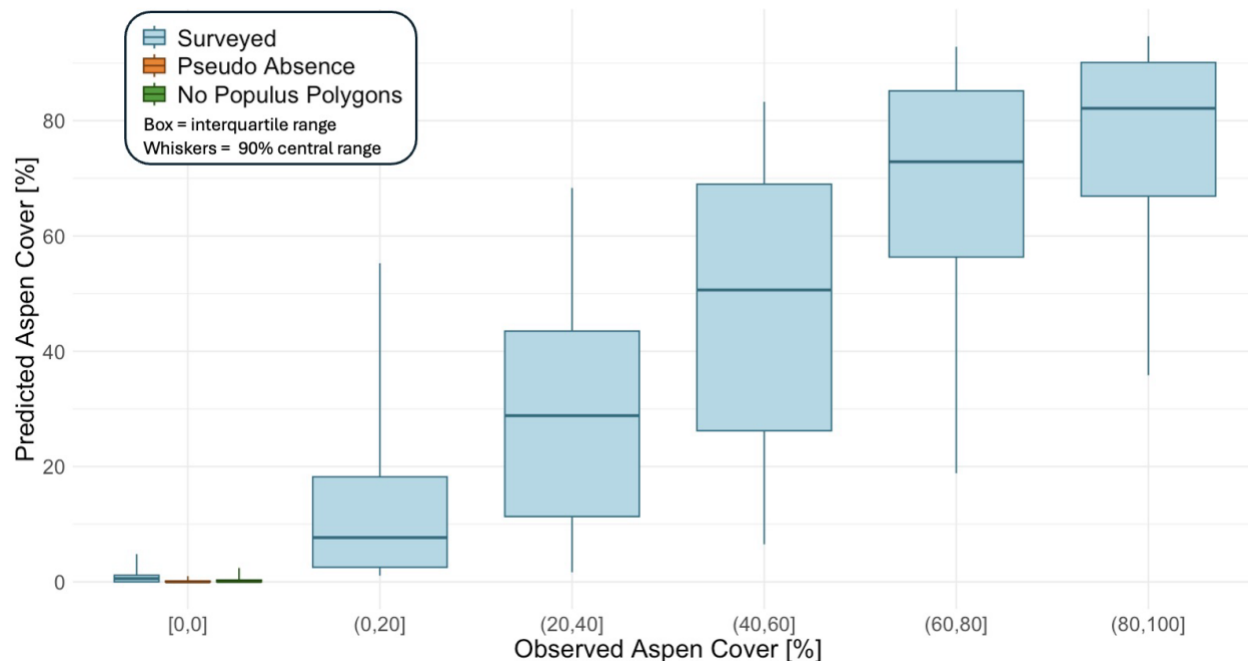


**Fig 3.** Reliability diagram depicting out-of-sample predictive performance of our ensemble model. The model appears to perform remarkably well distinguishing areas with aspen stands from areas without aspen stands and moderately well predicting aspen cover within individual 30-m x 30-m grid cells.

Compared with previous maps our ensemble model provides a more information rich picture of aspen cover. While our product provides quantitative estimates of aspen cover within 900-m<sup>2</sup> pixels, the previous maps classify polygons by vegetation type or taxa and do not estimate aspen cover with polygons. To the extent that these disparate data types can be compared, our product appeared to outperform the previous products. Still, there are locations that our product missed, and a previous product hit its target.

We compared our map with previous products by reviewing areas of disagreement between the products. We examined sequences of Google Earth imagery and conducted informal field surveys in these areas. Compared to previous maps, our map appeared to have higher overall levels of accuracy and detail. Our product appeared to be much more accurate than FVEG WHR (FRAP 2015). The two WHR types that explicitly include aspen are called “aspen” and “montane riparian”. FVEG had high rates of omission errors and moderate rates of apparent commission errors for identifying aspen stands. The FVEG map appears to omit a high proportion of aspen stands in our study area. We identified 925 ha where our ensemble model estimated aspen cover was > 25% but were not mapped as aspen or montane riparian types by FVEG, and 2,200 ha where our model estimated aspen cover was > 10% but were mapped as non-aspen types by FVEG. The WHR types that were most often misclassified as non-aspen types include juniper, montane hardwood-conifer, fresh emergent wetland, and lodgepole pine (Fig 4).

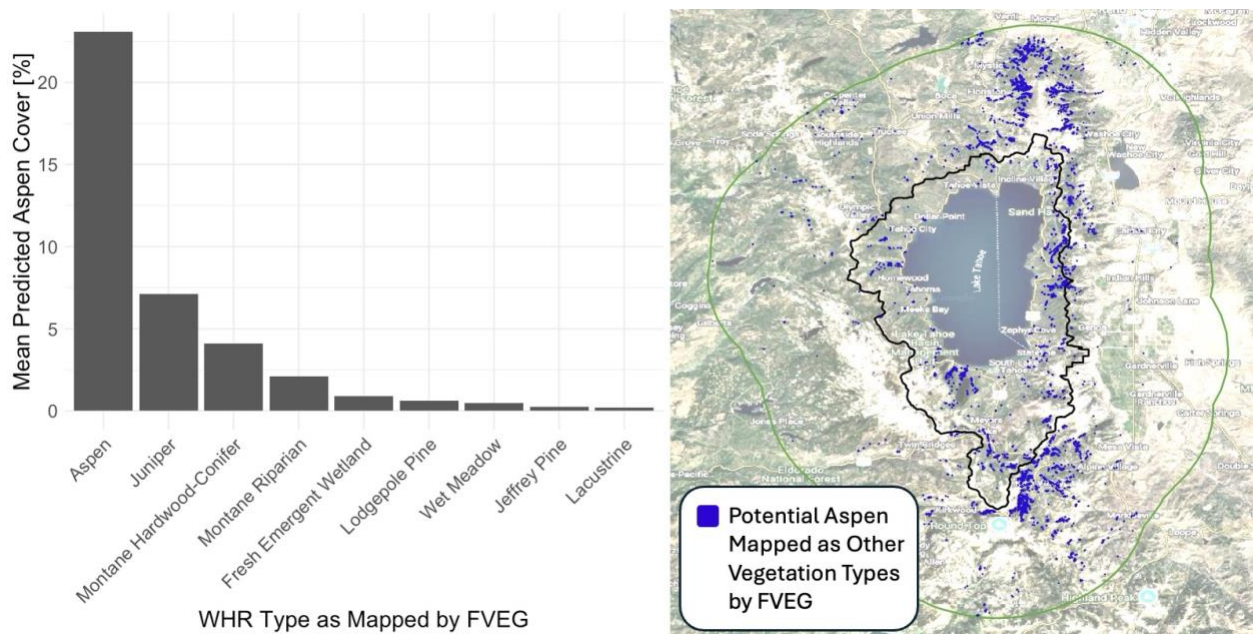


**Fig 4.** Discrepancies between our product and WHR vegetation type as mapped by FVEG. *Left panel:* Mean aspen cover, as estimated by our ensemble model, within areas mapped as WHR types by FVEG. Only the aspen and montane riparian WHR types explicitly include aspen in their type descriptions. Review of aerial imagery in areas of disagreement between the two products suggests that our product is much more accurate. In the FVEG map, WHR types that had a high proportion of aspen omission errors included juniper and montane hardwood-conifer types. *Right panel:* Locations predicted to have > 25% aspen cover by our model that are classified by FVEG as WHR types that do not explicitly include aspen. Location boundaries are outlined in blue to enhance their visibility.

Compared with FVEG WHR, the Dilts et al. (2020) map had far lower levels of both omission and commission errors. However, the Dilts et al. (2020) map appeared to be sometimes inconsistent in its level of spatial detail; some polygons have detailed boundaries that mostly exclude non-aspen areas, while some polygons include large areas (e.g., > 1 ha) where aspen are not apparent (*i.e.*, apparent commission errors). Our ensemble model appears to perform better at correctly identifying the presence of aspen than the Dilts et al. (2020) map, but both products are useful for finding errors made by the other product. Our product identifies many small aspen stands that were omitted by the Dilts et al. (2020) map. The Dilts et al. (2020) map includes many areas of sparse (e.g., 5%) aspen cover that were omitted by our product.

## Spatiotemporal Models

Annual to decadal temporal resolution models were fit for periods from 1984–2023. We evaluated modeling approaches that either pooled data over multiple year–year periods or fit models separately for each period. Of these two categories, models fit separately to each period performed better. Interannual differences in weather and phenology appear to result in distinct vegetation signals for each year–year period. Within the limited number of models we tested, models fit to one year–year period did not tend to generalize well to other periods. However, we anticipate that the predictive performance of pooled-period approaches can be improved with

further model tuning and data collection. Hybrid and/or hierarchical modeling approaches appear poised to result in improved performance for estimates of vegetation cover over time.

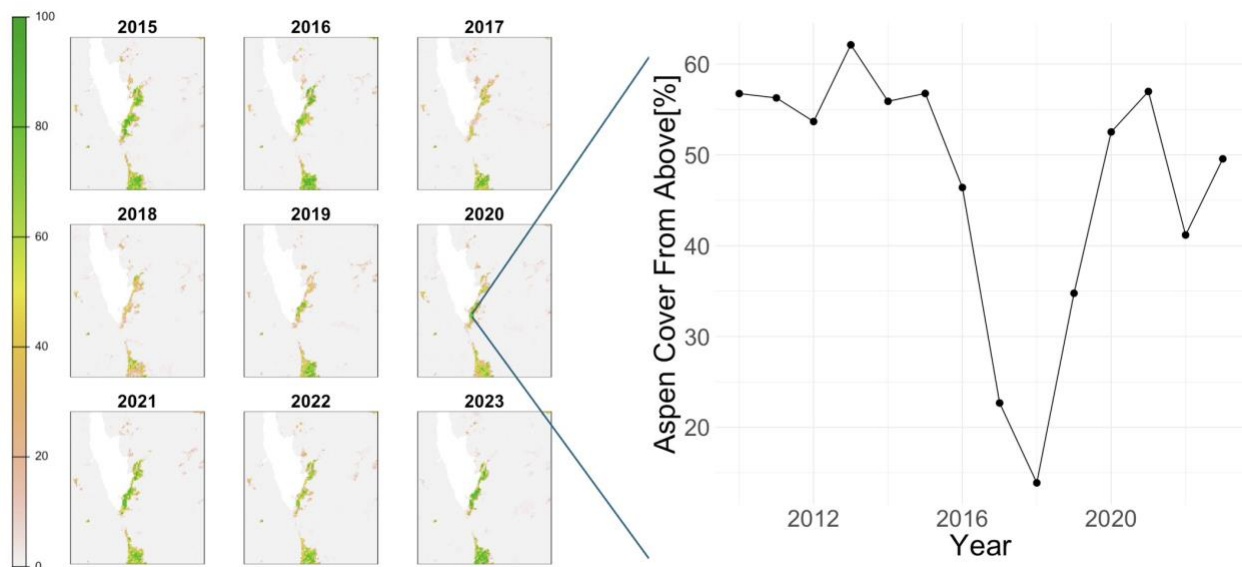


**Fig 5.** Model estimates of aspen decline and recovery around Marlette Lake during a mass summertime defoliation event caused by an outbreak of white satin moths. Model estimates of aspen cover over time broadly align with both written accounts and observations from NAIP and Google Earth imagery. Less clear is the degree to which year-to-year fluctuations before the mass defoliation event and after recovery reflect real ecological changes or statistical artifacts.

Machine learning models fit separately to each period demonstrated skill tracking clear cases of large-scale changes in aspen cover over time. For instance, model predictions generally tracked the mass defoliation and recover event surrounding the *circa* 2017 white satin moth outbreak at Marlette Lake (Fig 5), in which a large proportion of aspen trees lacked leaves during the summer growing season. At Marlette Lake, model estimates generally align with both written accounts and with clearly observable patterns in the sequence of Google Earth imagery. Similarly, model predictions for an area of the 2021 Tamarack Fire that burned at high severity align with a die-off event that is clearly observable from Google Earth imagery (Fig 6).

To assess the ability of our model to accurately track changes over time at local spatial scales more broadly we used linear regression on annual predicted aspen cover over time for each 900-m<sup>2</sup> pixel (*i.e.*,  $\text{aspen\_cover} \sim \text{intercept} + \text{slope} * \text{year}$ ). We examined trends over various time periods (*e.g.*, 2004–2023, etc.) and identified clusters of pixels with higher coefficients of determination (*e.g.*,  $R^2 > 0.5$ ). We then examined Google Earth imagery in a few dozen of these areas predicted to have substantial change in aspen cover over time. This evaluation had mixed results. In most areas Google Earth Imagery was not of sufficient quality to determine if the model was correctly identifying trends. When Google Earth imagery allowed for trend identification, our model appeared to outperform random chance in predicting the direction of aspen cover change. However, this exercise left us with the sense that model estimates of change in cover over time may be noisier than estimates of cover across space, and that further model improvements would be prudent to improve its capability to inform local-scale management.

Several areas, where the model identified potential changes in aspen cover, appear to have experienced mass defoliation events, where a large proportion of the mature aspen trees within a stand were clearly missing their leaves in the middle of summer for one or more years. We suspect that defoliation events in our training data may be causing the model to overestimate aspen cover for defoliated aspen. Refining our training data with further surveys, focused on tracking change over time in individual pixels, and well stratified across both space and time, would improve the model's ability to track changes in cover over time. Further, we suspect that building a remote sensing algorithm specifically focused on identifying summertime mass aspen defoliation events would be fruitful. There appears to be an abundance of mid-summer images of aspen defoliation events on Google Earth that could be used to develop data to train this model. Using this complementary method to identify mass defoliation events (e.g., white satin moth, fire) and the extent to which stands subsequently recovered, could substantially improve our ability to track change in aspen cover over time.

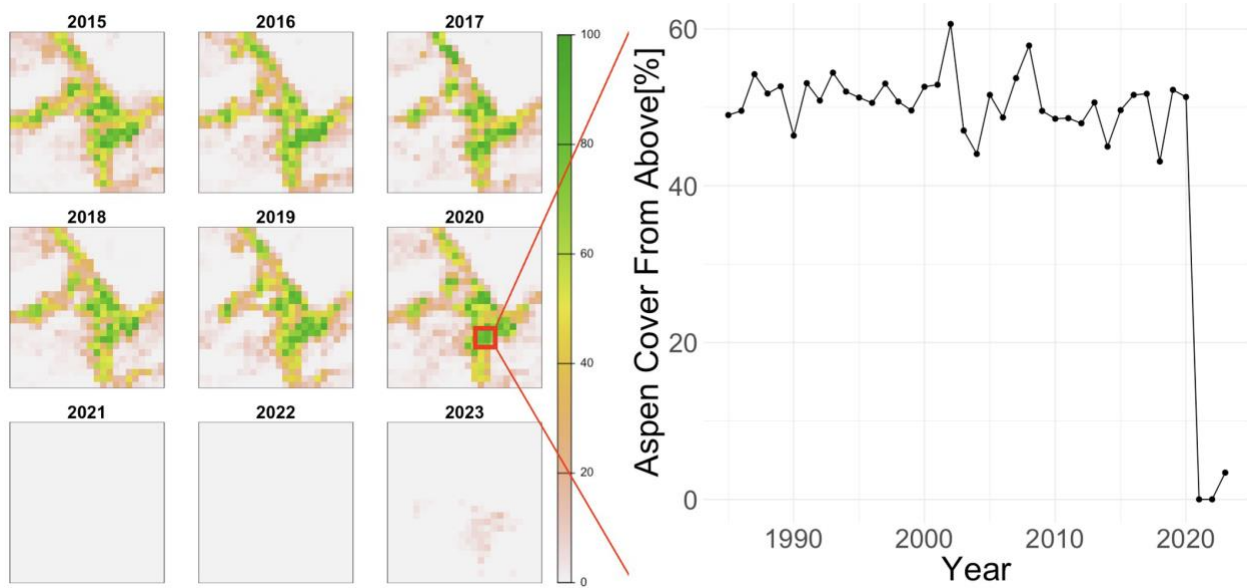


**Fig 6.** Aspen decline in an area of the 2021 Tamarack Fire that burned at high severity, followed by initial apparent recovery. Model estimates of aspen cover broadly align with observations from NAIP and Google Earth. The postfire recovery estimated by the model aligns with observations that aspen typically resprouts following high severity fire. However, because low-growing aspen saplings are more difficult to survey via aerial imagery than taller trees, on-the-ground surveys may be necessary to accurately train and validate model estimates of remotely sensed aspen recovery following high severity fire.

Our models appeared to have skill tracking aspen cover over time. However, we do not yet have sufficient repeated-measure survey data to quantify their accuracy in this task. Local estimates of change in cover over time may be noisier than estimates of cover across space, particularly where training data were sparser. We surmise that an expanded training dataset, focused on changes over time within individual plots, would improve and better quantify the model's ability to accurately track vegetation cover over time. Further model refinements are needed to more precisely and reliably track changes, particularly at finer spatiotemporal

resolutions. Users seeking to track change over time at local spatial scales should exercise caution interpreting the current version of our model estimates.

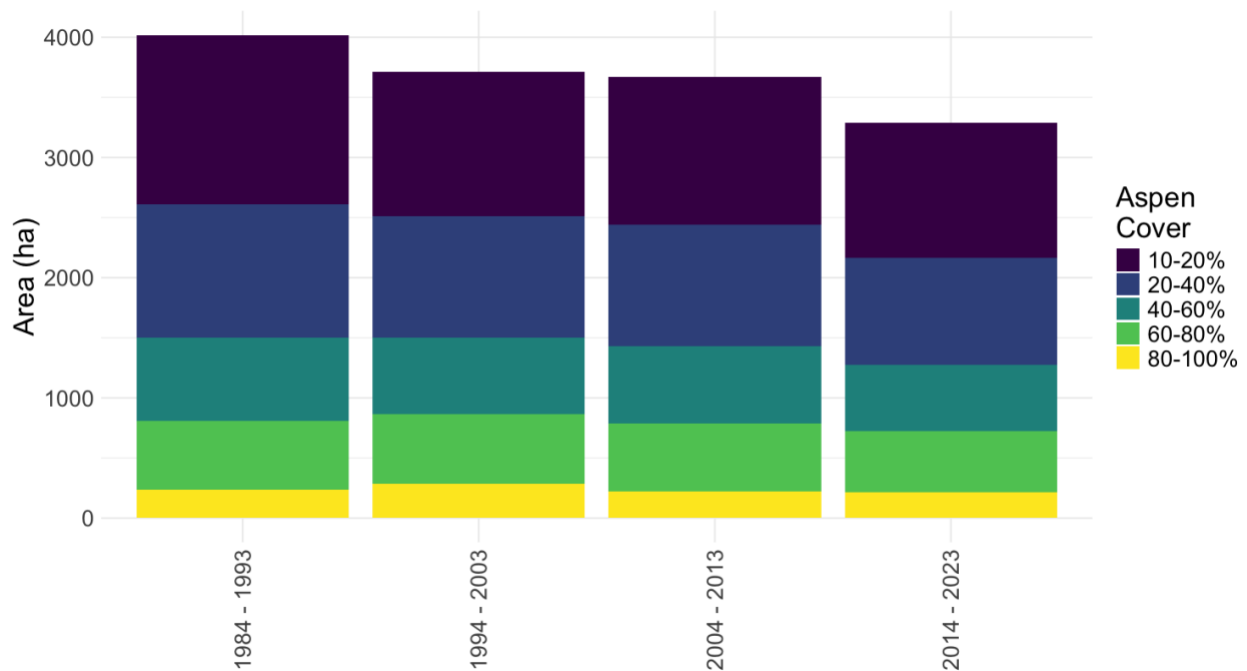


**Fig 7.** Estimated area by percent aspen cover within the broader Lake Tahoe area over time. The general trend of declining aspen cover over time is consistent across distinct versions of the model (e.g., distinct parameterizations for each period vs. pooled data over all periods; 1-, 2-, 5-, and 10-year periods, etc.). This figure depicts estimates from version 4.6.LS4to7.XGB of the model. We used only data from Landsat 4–7 here to avoid potential for shifting biases over time caused by inclusion of data for Landsat 8–9, which has slightly different spectral bands and begins in 2013.

Model outputs consistently indicated a decrease in aspen cover over time (1984–2023) in our study area (Fig 7). We used two methods to obtain estimates of percent change in aspen cover over time. For both methods we estimated the total area of aspen cover in our study region for each period, which we calculated as  $\Sigma(\text{aspen\_PCFA}/100 * \text{grid\_cell\_area} * (\text{aspen\_PCFA} > 10))$ , excluding grid cells where estimated aspen cover was  $\leq 10\%$  (i.e., where commission errors become more prevalent). Both methods used only spectral data from Landsat 4–7 to avoid potential biases from including Landsat 8–9 (i.e., we used model version 4.6.LS4to7.XGB). In the first method we simply calculated the ratio of the total area of aspen cover between the first (1984–1993) and last (2014–2023) 10-yr periods. This method yielded an estimated decline in aspen cover of 16%. In the second method we used log-linear regression on 5-yr resolution estimates of the total area of aspen cover. This method yielded an estimated decline of 26% (95% CI: 9–39%) over the 1984–2023 period.

One potentially confounding factor that could bias model estimates is the quantity or quality of Landsat spectral data. More limited availability of spectral data can cause the model to make more commission errors, resulting in higher estimates of aspen cover. If the quantity of spectral data increased over time, this could bias the model toward estimating a decline in

aspen cover. To mitigate this issue, we examined predicted aspen cover over time using only data from Landsat 4–7, thereby reducing the quantity of spectral data after the 2013 launch of Landsat 8. Landsat 8 and 9 use slightly different spectral bands, introducing another potential source of bias. The quantity of unobstructed Landsat 4–7 data over time exhibits a hump-shaped relationship; the 1999–2011 period has about twice as many unobstructed observations per pixel per year compared to the preceding, 1984–1998, and subsequent, 2012–2023, periods, which have about the same number of unobstructed observations per pixel per year. Estimates of change over time from models that used only Landsat 4–7 data show somewhat attenuated decline over time compared to models that used Landsat 4–9, but still estimate that substantial decline has occurred (Fig 7). Thus, while trends over time in the quantity of spectral data may bias our estimates of change in aspen cover over time, the qualitative trend of declining aspen cover over time was robust to this potentially confounding factor.

Another potentially confounding factor that could bias model estimates is change in aspen cover over time within our training data. For most of the plots in our dataset we assumed that aspen cover did not change over time. Exceptions included the area near the Marlette Lake, where a well-documented mass summertime defoliation event occurred circa 2017, and a small number of areas that experienced > 10% loss of basal area due to fire. If aspen cover tended to increase over time within our training data, this could bias the model to overestimate aspen cover during earlier periods. To mitigate this issue, we also examined trends in aspen cover using an earlier, pooled-period version of our model (version 4.1), where data from all periods was fed into a single machine-learning model parameterization and the single model was used for estimating aspen cover across all periods. Compared with later versions that parameterize the model separately for each period, this version of the model was less accurate. However, because the model parameterization does not change over time, the model has less potential to be biased by gradual changes in aspen cover within plots in our training data. Outputs from this pooled-period version of the model also indicated that aspen cover has decreased over time within our study area. Similarly, outputs from versions of our model that used 1-, 2-, 5-, and 10-year temporal resolution all indicated that aspen cover has declined. Notably, observations from field surveys and aerial imagery suggest that the opposite bias may be present; our training data appears to include plots where aspen cover decreased over time. For this reason, our current methods may underestimate the true rate of decline in aspen cover over time.

## Discussion and Management Implications

Our study provides an assessment of aspen (*Populus tremuloides*) distribution, cover, and change over time in the broader Lake Tahoe area over the past four decades. The high-resolution maps produced by our ensemble machine learning model offer a detailed picture of aspen cover, significantly improving upon previous vegetation mapping efforts in the region, which estimated aspen distribution but not the level of aspen cover. Our findings suggest a concerning trend of aspen decline, estimated at approximately 26% decline (95% CI: 9–39%) over the period from 1984 to 2023. This decline aligns with broader patterns observed across the western United States and highlights opportunities for targeted management interventions.

The ensemble model developed in this study demonstrated strong predictive performance ( $R^2 = 0.81$ ) in estimating aspen cover across the study area. The model's ability to detect aspen intermixed with various vegetation types and understory conditions is particularly noteworthy, given the limited training data (approximately 1,000 aerial surveys of 900-m<sup>2</sup> plots with non-zero aspen cover). This performance underscores the potential of machine learning approaches in vegetation mapping, especially when combined with strategic sampling and diverse data. Additional data and model refinements would increase the accuracy of model estimates across both space and time.

The model also demonstrates capacity to track changes in aspen cover over time. Its performance tracking known disturbance events, such as the white satin moth outbreak at Marlette Lake and high-severity wildfire impacts, provides evidence of the model's ability to quantify cover changes. Nevertheless, users should exercise caution when interpreting fine-scale estimates of change over time from our current models. Local-scale estimates of change in cover over time appear to be noisy; and we do not yet have sufficient repeated-measure survey data to more broadly quantify the accuracy of model estimates of change over time. Though local-scale estimates of change over time appear to be noisy we have greater confidence in region-wide estimates of change over time.

The estimated 26% decline in aspen cover over the past four decades is consistent with observations from other parts of the western United States (Pierce and Taylor 2010, Estes 2016, Refsland and Cushman 2021). This trend is particularly concerning given the ecological importance of aspen in the Lake Tahoe Basin, where it has been identified as one of nine Ecologically Significant Areas that disproportionately support biodiversity relative to their area (Murphy et al. 2000). Several interacting factors may be contributing to this decline. Fire suppression hinders aspen regeneration and facilitates conifer encroachment (Krasnow and Stephens 2015). This mechanism was apparent during our informal field surveys; we found areas where mature aspen stands appeared to have been recently replaced by dense conifers overtopping aspen understories (*i.e.*, fallen trunks of large aspen trees were prevalent on the ground). The recent invasion of white satin moths (*Leucoma salicis*), first detected in the Tahoe region in 2011, caused large-scale defoliation events in 2017 and 2018 (Tahoe Environmental Research Center 2019). Aspen declines have also been attributed to climate change, with further declines projected, unless there is a substantial increase in fire frequency (Rehfeldt et al. 2009, Yang et al. 2015, White et al. 2022).

Recent conifer thinning treatments in the basin alone appear unlikely to stem aspen declines because of their limited extent and limits on the size and amount of conifer trees that have been removed (Berrill et al. 2016, Berrill et al. 2017). Prospects for slowing or reversing aspen decline appear to hinge primarily on fire, specifically management of naturally ignited fires or higher-severity prescribed fires. Removal of conifers can boost regeneration but is less effective than fire. Aspen regeneration is more vigorous following high-severity wildfires than after low-severity burns or prescribed fires. Fire also creates conditions conducive to dispersal via seedling establishment. For this reason, fire may be crucial for aspen resilience to climate change because it creates opportunities for aspen to shift their distribution toward more favorable climate conditions. Strategic management of fire appears to be critical to maintaining and restoring aspen populations (Krasnow and Stephens 2015, White et al. 2022). Detailed maps of aspen cover—such as our product—can aid strategic and adaptive management,

allowing managers to steer fire for beneficial effects and target treatment to where they may be most effective. Our product may also be useful for identifying areas where conifers are suppressing aspen understories (e.g., where aspen cover has declined), though further model development would be prudent to improve this capacity.

## Methods

### Sample Design & Data Collection

We used human interpretation of vegetation cover from remote imagery to develop a dataset to train machine-learning models. Remote imagery consisted of aerial photographs (i.e., Google Earth, drone flights, NAIP), and publicly available ground-based photographs (e.g., Google Street View). Drone flights, focused on collecting high resolution images during the fall leaf-senescence period were conducted by Derek Young in October of 2023. Surveyors used these images to estimate vegetation cover within 900-m<sup>2</sup> square plots, aligned to USGS Landsat pixels. Our study area consisted of the broader Lake Tahoe Area (BLTA), defined by the Lake Tahoe Basin Management Unit (LTBMU or “the basin”) buffered by 20 km. USGS Landsat imagery in our study area spans raster grids in two projections: UTM zones 10N and 11N, with resolutions of 30-m and origins of (15,15). We processed these raster grids into two vector-based sampling grids, spanning our study region, for surveyors to overlay on top of aerial imagery.

UTM_Zone	PlotID	total check sum	tree check sum	Tree	shrub checksum	Shrub	Herbaceous	Non-Veg	Conifer	Cover From Above [%]	hardwood check sum	Populus tremuloides	Populus trichocarpa/fremontii	Cercocarpus ledifolius	Quercus kelloggii	Quercus waltzen/drydenii	Salix spp. (Tree, Shrub)	Sage, spp. (Shrub)	Alnus incana	Alnus monticola (Tree)	Alnus incana spp. lanulobila (mountain alder, Shrub)	Acer glabrum	Overhead Image Source	Overhead Image Date	Ground Image Source	Ground Image Date	Interpreted By	Notes	
11	3012392	100	92	92	0	1	2	5	8	84	84																		
11	1839866	100	48	48	0	47	5		1	47	47											47	Google Earth	4/16/2015	NA		LYH	This was a particularly easy plot for estimating veg cover, and	
11	1844519	100	96	96	0		4		0	96	96												Google Earth	4/16/2015	NA		LYH	Leaf on image (6/23/2016) and Leaf off (4/16/2015). This was	
11	2819162	100	55	55	0	22	19		4	17	38	38											Google Earth	4/16/2015	NA		LYH	Leaf on image (6/23/2016) and Leaf off (4/16/2015). [sample	
11	2741107	100	50	50	0	46	4		21	29	29	29										46	Google Earth	4/29/2014	NA		LYH	Leaf on image (6/23/2016) and Leaf off (4/29/2014). Best view	
11	2746820	100	92	92	0	6	2		19	73	73	73											Google Earth	4/29/2014	NA		LYH	Leaf on image (6/23/2016) and Leaf off (4/29/2014). [sample	
11	2746821	100	88	88	0	12			25	63	63	63											Google Earth	4/29/2014	NA		LYH	Leaf on image (6/23/2016) and Leaf off (4/29/2014). [sample	
11	3414968	100	29	29	0	30	41		1	28	28	28											Google Earth	6/22/2016	NA		LYH	Leaf on image (6/23/2016) and Leaf off (4/16/2015). [sample	
11	3416112	100	70	70	0		30		27	43	43	43											Google Earth	7/13/2016	NA		LYH	Leaf on image (7/13/2016) and Leaf off (4/16/2015). [sample	
11	982006	100	74	74	0	3	23		11	63	63	63											Google Earth	6/7/2018	NA		LYH	Leaf on image (6/7/2018) and Leaf off (4/29/2014). [sample C	

**Fig 8.** A screenshot of our initial vegetation survey database and data entry form. A subsequent version of this form includes a range of dates, instead of a single date, for which surveyors assess vegetation cover estimates to be accurate.

We developed a vegetation survey protocol in collaboration with Laura Young-Hart (LYH), of the Mapping and Remote Sensing Program at the US Forest Service. LYH is a botanist with strong expertise and experience surveying vegetation via aerial imagery for mapping and assessment. LYH helped us identify which tree and shrub taxa can be reliably identified by human observers using aerial imagery. We identified five physiognomic groups and ten native hardwood taxonomic groups that are common in our study region and can be readily identified by skilled observers. Physiognomic categories included conifer tree, hardwood tree, shrub, herbaceous, and non-vegetation. The most readably identifiable taxonomic groups in our study area include: *Populus tremuloides* (quaking aspen), *Populus trichocarpa/fremontii* (black and Fremont cottonwoods, which are difficult to distinguish in part because they commonly hybridize in the region forming *Populus x parryi*), *Cercocarpus ledifolius* (mountain mahogany),

*Quercus kelloggii* (California black oak), *Quercus wislizenii/chrysolepis* (interior and canyon live oak), *Salix spp.* (tree willows), *Salix spp.* (shrub willows), *Alnus rhombifolia* (white alder), *Alnus incana spp. tenuifolia* (shrubby mountain alder), and *Acer glabrum* (Rocky Mountain maple).

The survey protocol consists of first visually scanning aerial and ground-based imagery to find plots where vegetation cover can be identified with high confidence. Typically, this involves finding regions where vegetation is clearly visible and can be viewed in multiple seasonal conditions (e.g., spanning the range from winter leaf-off conditions to autumn leaf senescence). Once clearly identifiable plots were selected, surveyors estimated percent cover from above (PCFA) for each physiognomic and taxonomic group (Fig 8). Each survey includes a date, or range of dates, for which the surveyor believes their PCFA estimates are accurate. We added date ranges to the survey protocol late in our data collection effort, to better support parameterization of models with higher temporal predictive accuracy. These included repeated surveys of 63 plots where changes in vegetation cover over time were evident. We recommend that any similar future efforts begin with date ranges and repeat measures instead of a single survey date for each plot.



**Fig 9.** Three Google Earth images of the same Landsat-aligned plot (red boundaries) containing mature aspen trees and a large conifer. Leaf-off images can be particularly diagnostic for identifying mature aspen, revealing their light-colored stems. Distinctive branching patterns are especially apparent from oblique views (right) and from shadows on the ground (left). Images of spring green-up and autumn leaf-senescence (not shown) can also be diagnostic but are less abundant in our study region.

LYH spearheaded data collection efforts by collecting vegetation cover data for about 80 plots. A primary objective here was to provide characteristic examples of a range of hardwood species, identified by an expert, for use in training other vegetation surveyors. We contracted with SIG-NAL to conduct the rest of the surveys for this project, to be performed by workers with strong experience surveying vegetation via aerial imagery. Despite the examples provided by LYH, SIG-NAL surveyors found identifying non-aspen hardwood species challenging and time consuming. Aspen is the most abundant hardwood tree species in the basin, one of the most important species from a biological conservation perspective (the Lake Tahoe Watershed Assessment (Murphy and Knopp 2000) identified aspen groves as one of 9 Ecologically Significant Areas that disproportionately support biodiversity relative to their area), and one of the easiest to distinguish via aerial imagery (Fig 9). Therefore, to enhance the odds that we

could produce maps that address identified management needs, we prioritized collection of aspen cover data (Fig 10). We hoped that SIG-NAL surveyors would become more confident identifying the other hardwood species over the course of their work and that they would have sufficient time to estimate cover for additional hardwood species. To increase our sample size, we reallocated some of the UC Davis funding to hire an additional surveyor, which proved to be cost-effective, as the UC Davis surveyor completed more than ten times as many surveys per dollar spent compared with SIG-NAL (Table 2). While the surveyors employed by SIG-NAL did high quality work, they were considerably more expensive.

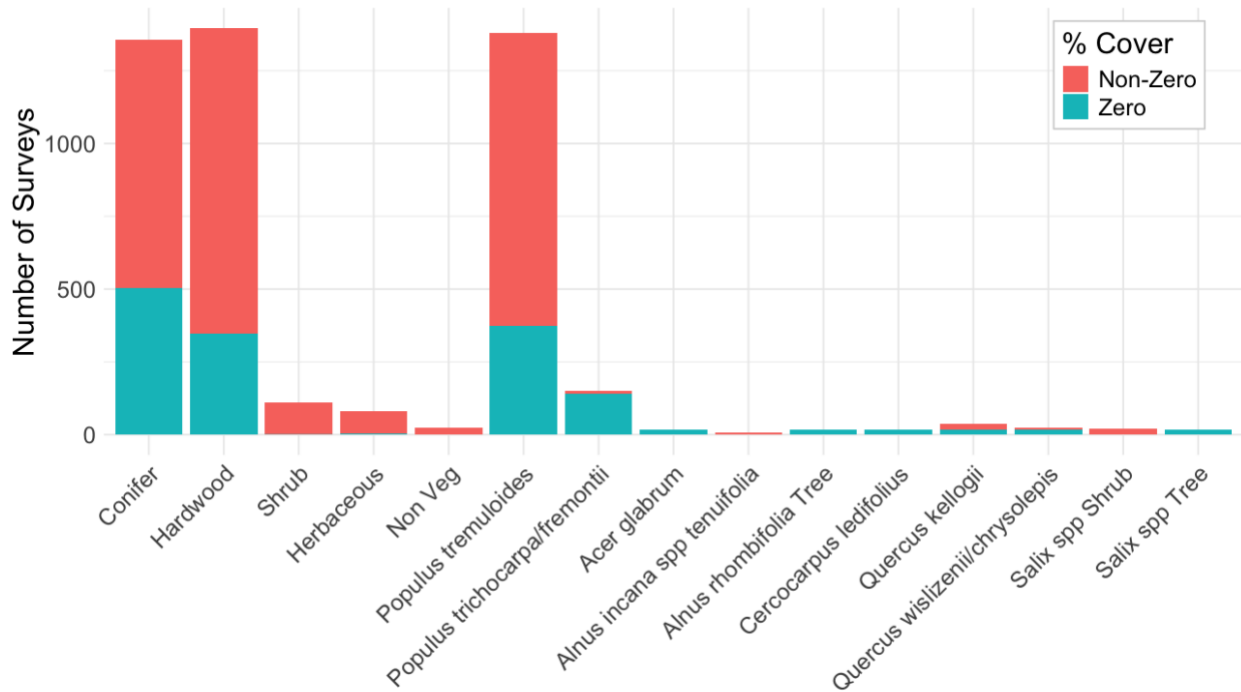


**Fig 10.** Number of surveys of 900-m<sup>2</sup> Landsat-aligned plots with percent-cover-from-above estimates for each physiognomic and taxonomic group. Most surveys where non-zero cover was estimated for non-aspen hardwood taxonomic groups were conducted by LYH (see text). The dearth of non-zero cover estimates for non-aspen hardwood taxa precluded us from developing useful maps for additional taxa.

**Table 2.** Number of surveys conducted as part of this project by survey team.

Survey Team	900-m <sup>2</sup> Plot Surveys	No- <i>Populus</i> Polygon Surveys
SIG-NAL	927	3
USFS	188	77
UC Davis	290	0
<b>Total</b>	<b>1,405</b>	<b>80</b>

Over the course of data collection, we held weekly coordination meetings with surveyors. We attempted to balance survey efficiencies that are gained by surveying several nearby plots with spreading out surveys sufficiently to reduce spatial autocorrelation in our sample. We also sought to stratify surveys across climatic gradients, to capture variability in phenological spectral signals, and gradients in taxon-specific vegetation cover (Fig 11). The following quality control measures were taken. Plots with potentially confusing images or from potentially confusing

contexts were reviewed as a group (e.g., shrubby aspen growing on poor substrate). We used out-of-sample preliminary model predictions (see model parameterization) to identify potential transcription errors in vegetation cover data. We individually reviewed plots with large discrepancies between recorded and predicted aspen cover and asked surveyors to re-assess a subset of these plots. Similarly, we identified plots with impossible combinations of data (e.g., aspen cover estimated to be higher than total hardwood cover). Upon re-assessment, we corrected plots that had data-entry errors.

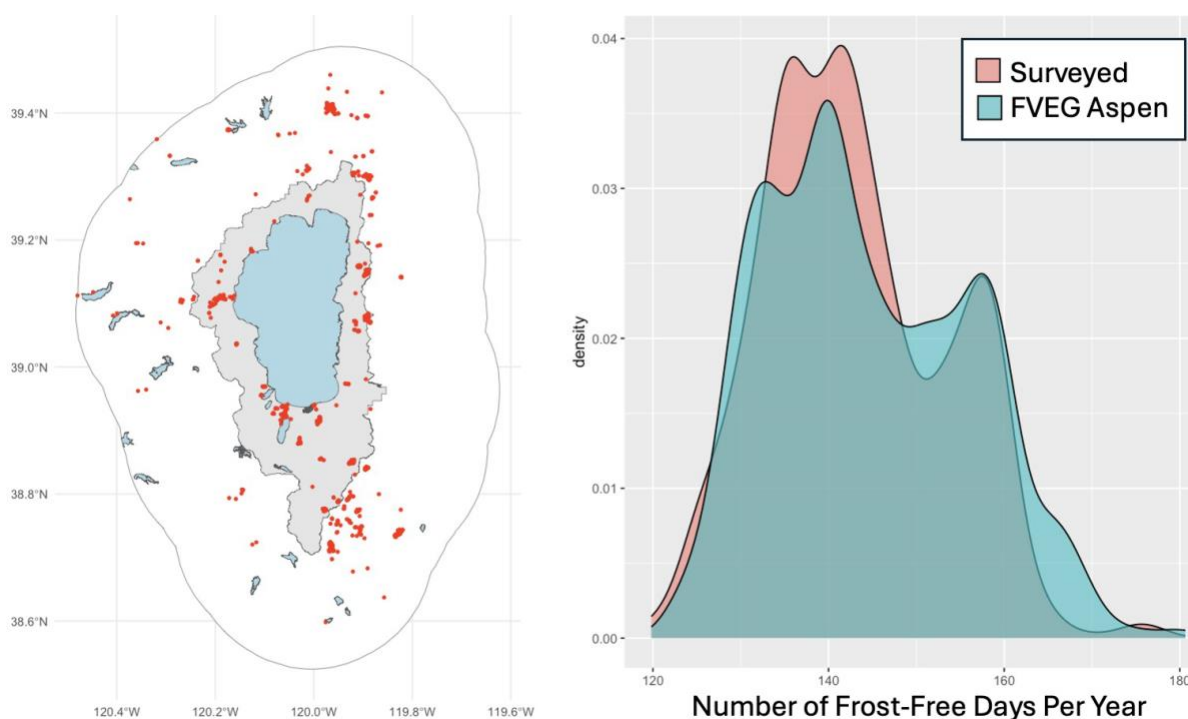


**Fig 11.** Spatial and climatic distribution of survey data collected by this project. *Left panel:* Survey locations are shown in red. The Lake Tahoe Basin Management Unit (LTBMU) is shown in grey. The boundary of our study region, the broader Lake Tahoe Area (BLTA), is a 20-km buffer around the LTBMU and shown as a black outline. Major lakes are shown in blue. *Right panel:* Our sampling density with respect to number of frost-free days per year, a proxy for the duration of the growing season, approximates the distribution of aspen as previously mapped by FVEG within our study area, with a notable dearth of plots from areas with longer growing seasons (*i.e.*,  $\geq 165$  frost-free days per year).

The consensus among surveyors was that larger aspen trees are easily identifiable via aerial imagery, while lower growing aspen is challenging to identify even when aerial images are entirely unobscured by taller trees. Ground-based imagery did support confident identification of low-growing aspen, though these images (e.g., google street view) were less available. As a result, our survey method biases our sample away from including plots with low-growing aspen. Aspen stands may be low growing because they are young, but aspen also commonly have a short, shrubby stature where they grow on suboptimal substrates (e.g., talus) in the study area. To the extent that the spectral and phenological signals of low growing aspen differ from larger aspen trees, this could bias our mapped outputs to under-detect low-growing aspen, even when

satellite imagery is unobstructed by taller trees. However, our informal field surveys suggest our models generally perform well in identifying low-growing aspen.

Toward the end of our survey efforts, manual review of maps produced by preliminary machine learning models revealed remaining commission errors (*i.e.*, predicting aspen was present, typically at low cover, in areas where it clearly wasn't). To tamp down on these errors we asked surveyors to identify larger polygons where commission errors were present. Due to apparent similarity in spectral signals between aspens and cottonwoods, we asked surveyors to identify large polygons where neither aspen nor other *Populus spp.* were present, and where the model predicted > 5% aspen cover over a substantial portion of the polygon. We called this category of survey no-*Populus* polygons (NPP). From the NPPs we extracted a weighted random sample of 900-m<sup>2</sup> plots that were fully contained within the NPPs (*i.e.*, not spanning the edge of NPP boundaries) for model training. While commission errors remain, this approach greatly reduced the prevalence of commission errors.

Overall, our vegetation survey efforts resulted in 1,405 quality-controlled surveys of 900-m<sup>2</sup> plots, aligned to the USGS Landsat grid, and 80 large no-*Populus* polygons. 1,396 of the plot surveys include estimates of aspen cover. 197 plot surveys include estimated percent cover for at least one non-aspen hardwood taxa. 57 surveys include non-zero estimates of percent cover for at least one non-aspen hardwood taxa (*i.e.*, primarily collected by USFS). Due to the dearth of taxon-specific cover estimates for other hardwood species we were limited to producing maps of aspen cover only. Surveys span the period 2004 to 2023 and include 63 plots that were resampled over time, in areas where disturbance events were evident (Fig 12). The sampling density of 900-m<sup>2</sup> plots appears to closely approximate the distribution of aspen within our study area with respect to number of frost-free days per year, a climatic proxy for differences in the timing of aspen phenology (Fig 11). The sample has a notable bias toward inclusion of plots with higher (e.g., 70–90% cover) aspen cover, compared to plots with lower percent cover (Fig 13).

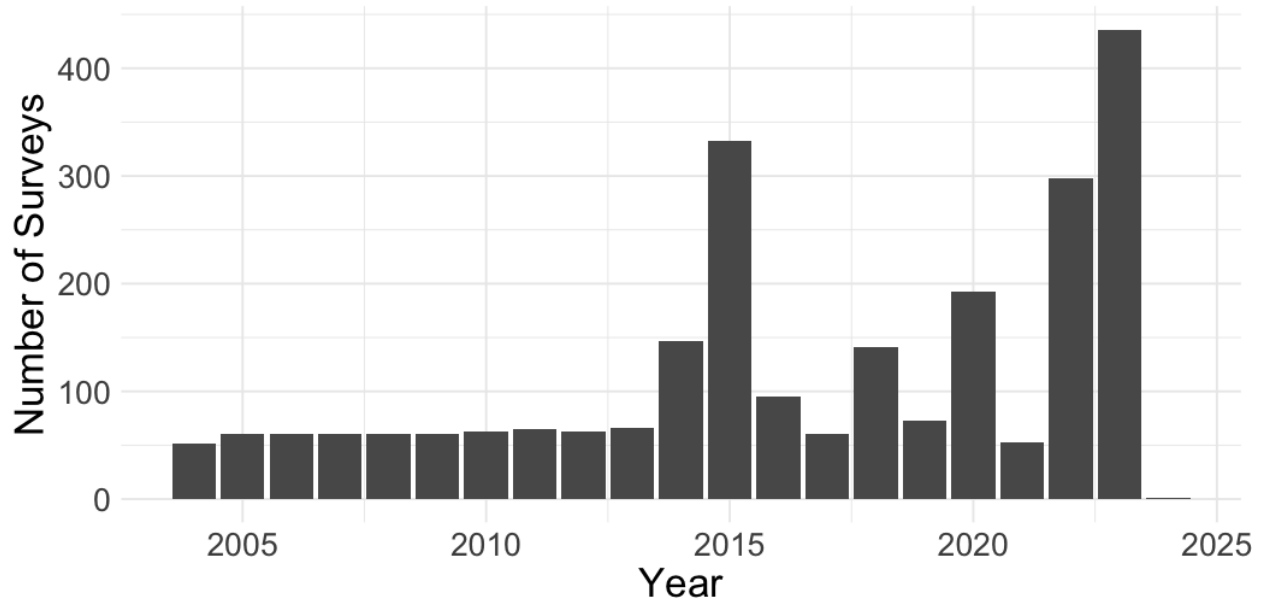


**Fig 12.** Number of surveys of 900-m<sup>2</sup> Landsat-aligned plots over time. Each survey included either a single representative date or a range of dates, for which the surveyor was confident in the accuracy of their vegetation cover estimates. The sample includes 63 plots that were sampled over multiple distinct periods (e.g., before and after substantial disturbances).

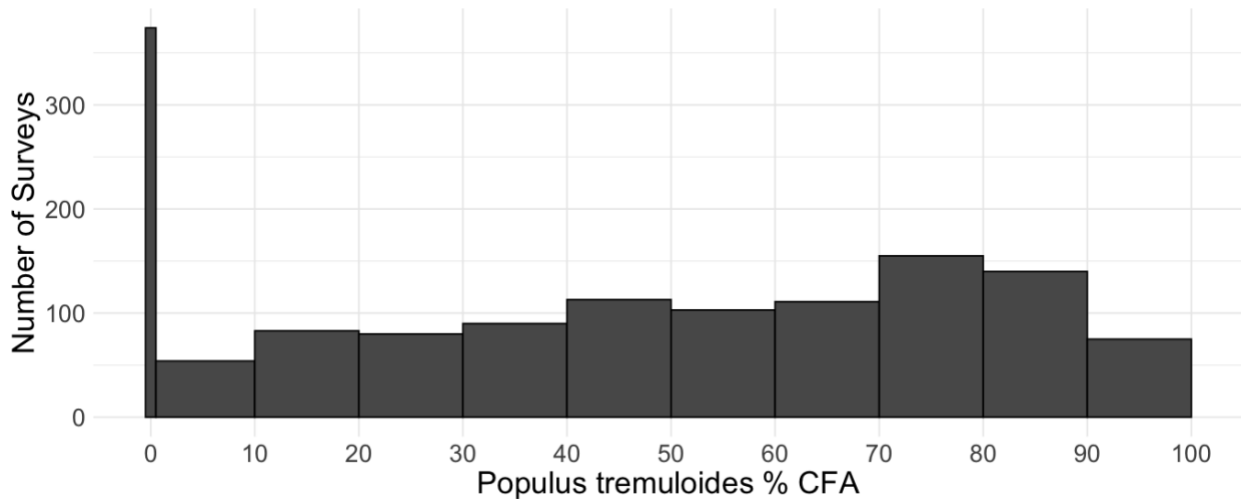


**Fig 13.** Histogram of Aspen percent cover from above in our sample of 900-m<sup>2</sup> Landsat-aligned plots.

## Reflectance Data

To capture phenological signals we categorized spectral data into distinct seasonal periods by calendar day of year. Spectral data was filtered to remove obstructions, including clouds, dilated clouds, cloud shadows, and surface water. We endeavored to balance the tradeoff between signal improvements associated with finer temporal resolution seasonal periods against reductions in the sample size of obstruction-free images. For models focused on estimating vegetation cover over longer, multi-year periods (e.g., for a five-year period, such as

2019–2023) finer temporal resolution (e.g., 15-day periods during the summer low cloud period, from day of year 165 to 330) tended to achieve higher cross validated predictive accuracy. For models focused on estimating vegetation cover over shorter annual periods (e.g., for a single year up to a few years) longer seasonal periods appear to be more appropriate.

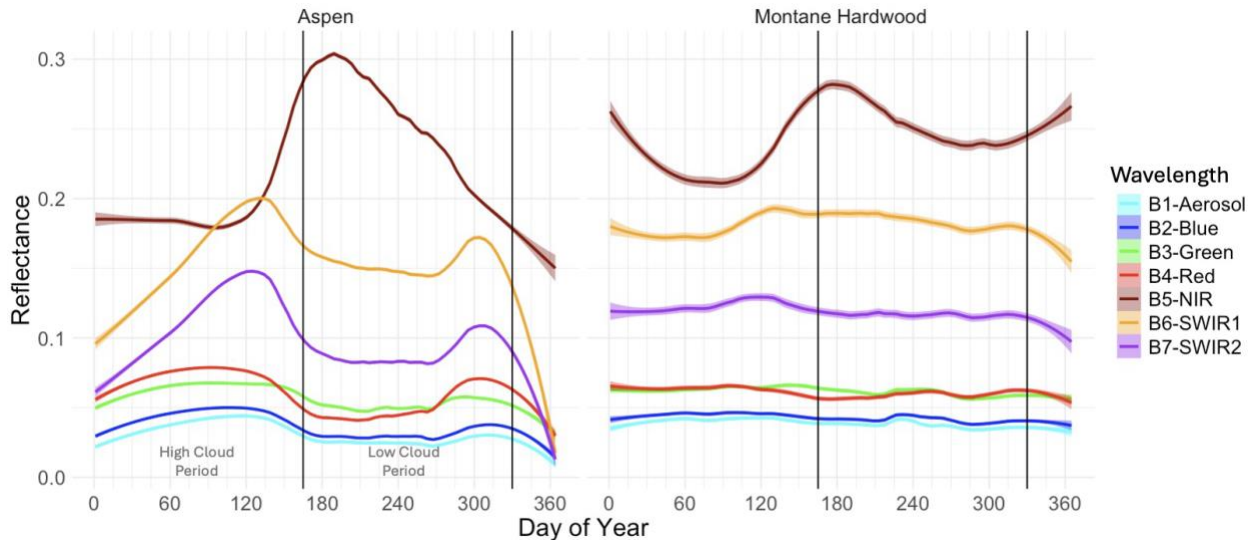


**Fig 14.** Phenological patterns in spectral signatures provide signals that can be used to identify vegetation composition from high-temporal resolution multi-spectral satellite imagery. Distinct phenological signatures both inside and outside of the low-obstruction period appear to be highly informative. The spring peak in short-wave infrared bands 6 and 7 around day of year 120 is frequently obstructed by clouds (Fig 15).

We obtained and processed gridded reflectance data from the USGS Landsat 4–9 Collection 2, Level 2, Tier 1 dataset using Google Earth Engine and R. To minimize data degradation, we maintained the data in its native USGS grid projections within our project area, which falls under UTM zones 10 and 11 (30-m resolutions, origins at 15, 15). Data was downloaded in tabular and raster formats. Tabular data consisted of unprocessed individual reflectance measurements and obstruction flags, for plots (*i.e.*, raster cells) where we had collected vegetation cover data. This time-series data was processed in R and used for initial model tuning. Raster data was processed into obstruction-free, median-over-time values covering our study area. Time periods consisted of combinations of up to 16 seasonal periods per year (e.g., days of year 165–180, etc.), with both annual and multi-annual (e.g., 2019–2023) periods. Spatially extensive raster data was used for final model parameterization and predictions. Compressed reflectance data occupy a couple hundred gigabytes of storage.

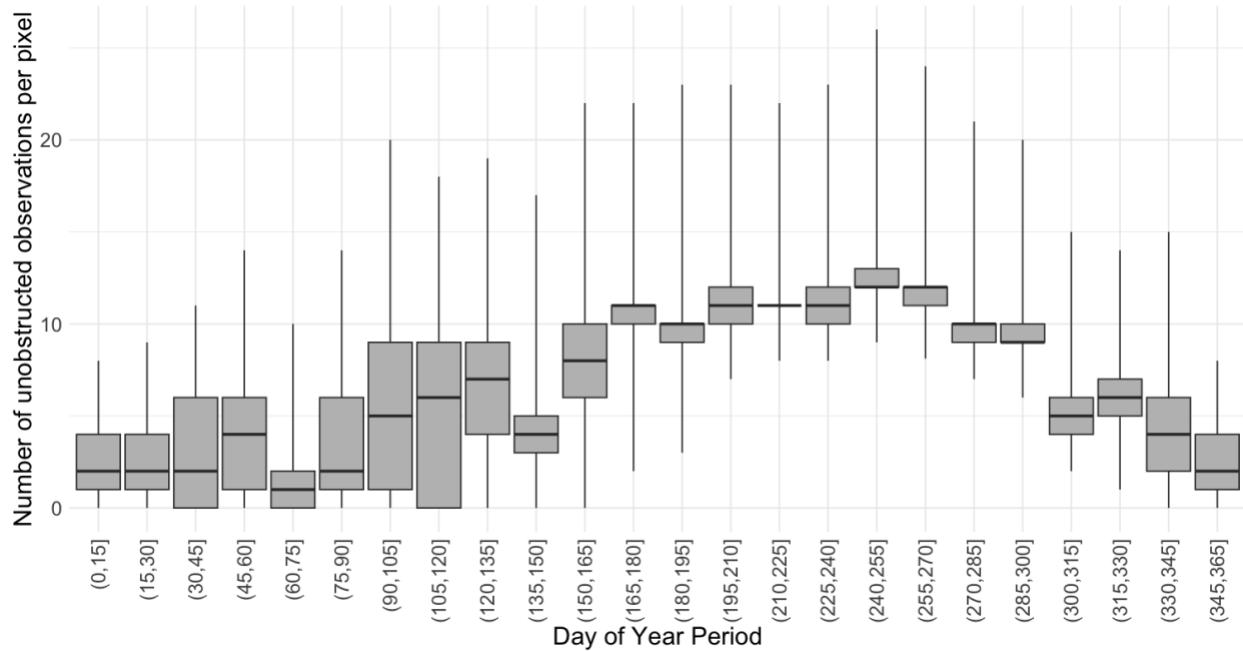


**Fig 15.** Number of unobstructed Landsat 8–9 observations per pixel in our study region by seasonal period, from 2013 to 2023. Boxes depict the median and interquartile range. Whiskers depict the 99% central range. Obstructions include clouds, dilated clouds, cloud shadows, and snow. The “low obstruction period” in our study region approximately spans the period from day of year 165 to 330.

## Model Parameterization

We combined three types of vegetation cover data for model training and validation. The first and most important category was surveys of 900-m<sup>2</sup> Landsat-aligned plots. The second category was background or “pseudo-absence” plots. Locations of about 40,000 background plots were randomly drawn from our study region. To increase the odds that background plots were not located within aspen stands, we discarded plots in, or within 60-m of, areas previously mapped as aspen or montane riparian types. The third category, no-populus polygons (NPP), was introduced last to tamp down on remaining commission errors that were apparent when manually reviewing model predictions against remote imagery. We provided vegetation surveyors with predicted maps of aspen cover and asked them to identify large polygons where they had high confidence that *Populus spp.* were not present and where portions of the polygons were predicted to have substantially greater than zero aspen cover. We then selected a weighted random sample of about 40,000 Landsat-aligned plots that were fully contained in (*i.e.*, not spanning the edge of) the NPPs.

We temporally aligned vegetation cover estimates with reflectance data. Fire severity was estimated using the CALFIRE fire perimeter database and methods from Parks et al. 2018 and Stewart et al. 2021. When moderate wildfire (*e.g.*, > 10% basal area loss) and other known disturbances (*e.g.*, white satin moth outbreaks) were not apparent, we assumed that vegetation cover remained relatively unchanged over time. The strength of this key assumption was iteratively tuned for different versions of the model (*e.g.*, vegetation cover was assumed to be constant for 1–15 years in absence of disturbance). Resulting model predictions were then

evaluated for their cross-validated predictive performance and as well as their accuracy when assessed with remote imagery and field surveys.

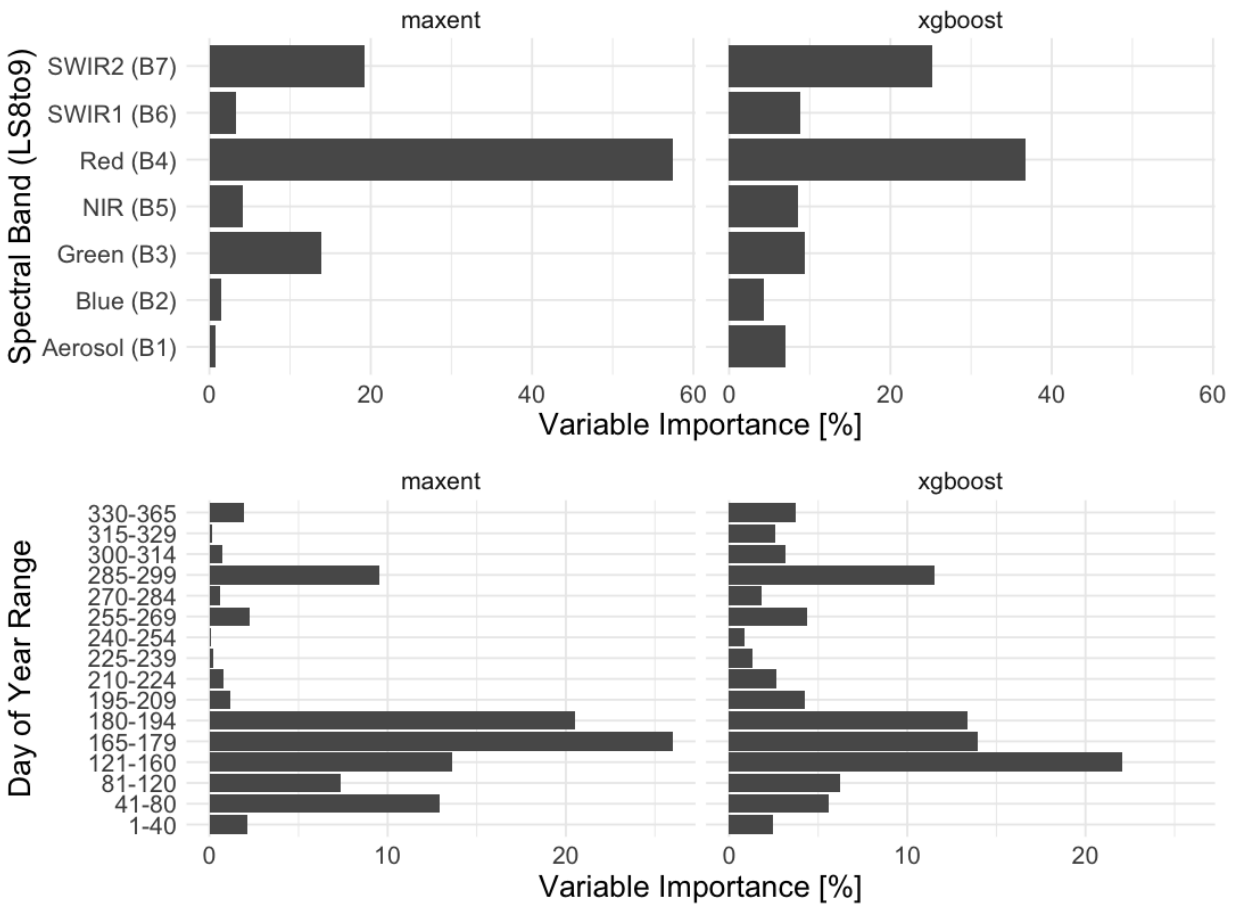


**Fig 16.** Importance of Landsat 8-9 imagery from different spectral bands and seasonal periods (day or year ranges) for predicting aspen cover for extreme gradient boosting and Maxent. Note that extreme gradient boosting reports higher importance for the spring period from day of year 121 to 160, when the spring green-up signal is often obscured by cloud cover, reflecting the XGB’s flexibility in accommodating missing independent data.

Of the many model-fitting algorithms we evaluated, extreme gradient boosting (XGB) and Maxent (ME) had the best cross validated predictive performance and the most plausible predictions when compared with remote photography. Hyperparameters for XGB were manually tuned by iteratively fitting models and examining cross-validated predictive accuracy and comparing predictions against aerial imagery. Maxent typically requires Bernoulli distributed (0-1) response variables; to transform percent cover estimates into binary data we disaggregated each individual binomial cover estimates into up to 100 Bernoulli-distributed values for the response variable (*i.e.*, 25% cover becomes 25 observations of 100% cover and 75 observations of 0% cover).

Between these two algorithms XGB is particularly useful due to its seamless ability to produce predictions when missing independent variables are present. This ability enables

incorporation of finer temporal resolution seasonal spectral data, where missing data may be present due to prevalence of obstructions such as cloud cover. The implication here is that XGB has superior ability to incorporate spectral signals that are sometimes obstructed, such as spring peaks in short-wave infrared bands 6 and 7 that are often obstructed by clouds (Figs 14, 15, 16). In contrast, feeding missing data into ME (e.g., one out of many seasonal periods has no obstruction-free spectral data) results in both discarding whole vegetation surveys from model parametrization and in missing (no data) areas on predicted maps of vegetation cover.



*Composite Image of Aspen in October 2023 by Derek Young*

## Contributors

Laura Young-Hart contributed to designing our vegetation survey protocol, conducting surveys, and advising other surveyors. Travis Freed and Nick Miley performed the bulk of 900-m<sup>2</sup>-plot vegetation surveys for this project. Jennifer O'Brien contributed to vegetation surveys. Derek Young conducted drone flights in October 2023 and assembled composite images. Quinn Sorenson contributed to initial data carpentry and model parameterization. Enikoe Bihari contributed to compiling previous vegetation maps.

## Supplementary Materials

Estimates of aspen cover in the broader lake Tahoe area over the period 1984–2023 are available at <https://stewartecology.org/TahoeAreaAspenMaps/>

## References

- Berrill, J.-P., Dagley, C.M., Coppeto, S.A. (2016). Predicting treatment longevity after successive conifer removals in Sierra Nevada Aspen Restoration. *Ecological Restoration*, 34(3), 236–244.
- Berrill, J.-P., Dagley, C.M., Coppeto, S.A., Gross, S.E. (2017). Curtailing succession: Removing conifers enhances understory light and growth of young aspen in mixed stands around Lake Tahoe, California and Nevada, USA. *Forest Ecology and Management*, 400, 511–522.
- California Department of Forestry and Fire Protection (CALFIRE), Fire and Resource Assessment Program (FRAP). (2015). *Forest Vegetation (FVEG) Database, version 15.1*. Retrieved from <https://frap.fire.ca.gov/mapping/gis-data/>
- Dilts, T.E., Williams, H.P., Refsland, T.K., Cushman, J.H. (2020). Lake Tahoe Basin Aspen Map of 2018, version 0.92 [Geospatial Data]. University of Nevada, Reno. Available at <https://nevada.box.com/s/o5lbh3eh939kb5yn9otaeetlo3rkd84>.
- Estes, B.L. (2013). Historic Range of Variability for Aspen in the Sierra Nevada and South Cascades. *Placerville, CA: Central Sierra Province Ecologist, Eldorado National Forest*. 47 p. Retrieved from [https://www.fs.usda.gov/Internet/FSE\\_DOCUMENTS/stelprdb5434340.pdf](https://www.fs.usda.gov/Internet/FSE_DOCUMENTS/stelprdb5434340.pdf)
- Krasnow, K.D., Stephens, S.L. (2015). Evolving paradigms of aspen ecology and management: impacts of stand condition and fire severity on vegetation dynamics. *Ecosphere*, 6(1), 12.
- Murphy, D.D., Knopp, C.M. (2000). *Lake Tahoe Watershed Assessment, Volume 1*. USDA Forest Service, Pacific Southwest Forest and Range Experiment Station General Technical Report PSW-175: Albany, CA.  
[https://www.fs.usda.gov/psw/publications/documents/psw\\_gtr175/](https://www.fs.usda.gov/psw/publications/documents/psw_gtr175/)
- Parks, S.A., Holsinger, L.M., Voss, M.A., Loehman, R.A., Robinson, N.P. (2018). Mean composite fire severity metrics computed with Google Earth Engine offer improved accuracy and expanded mapping potential. *Remote Sensing*, 10(6), 879.
- Pierce, A.D., Taylor, A.H. (2010). Competition and regeneration in quaking aspen-white fir (*Populus tremuloides-Abies concolor*) forests in the Northern Sierra Nevada, USA. *Journal of Vegetation Science*, 21, 507–519.
- Refsland, T.K., Cushman, J.H. (2021). Continent-wide synthesis of the long-term population dynamics of quaking aspen in the face of accelerating human impacts. *Oecologia*, 197, 25–42.
- Rehfeldt, G.E., Ferguson, D.E., Crookston, N.L. (2009). Aspen, climate, and sudden decline in western USA. *Forest Ecology and Management*, 258, 2353–2364.
- White, A.M., Holland, T.G., Abelson, E.S., Kretchun, A., Maxwell, C.J., Scheller, R.M. (2022). Simulating wildlife habitat dynamics over the next century to help inform best management strategies for biodiversity in the Lake Tahoe Basin, California. *Ecology and Society*, 27(2).
- Yang, J., Weisberg, P.J., Shinneman, D.J., Dilts, T.E., Earnst, S.L., Scheller, R.M. (2015). Fire modulates climate change response of simulated aspen distribution across topoclimatic gradients in a semi-arid montane landscape. *Landscape Ecology*, 30, 1055–1073.